Original Paper

phys. stat. sol. (b) **244**, No. 11, 3885–3889 (2007) / **DOI** 10.1002/pssb.200776174

Metallic bundles of single-wall carbon nanotubes probed by electron spin resonance

F. Simon[*, 1, 3], **D. Quintavalle**[1], **A. Jánossy**[1], **B. Náfrádi**[2], **L. Forró**[2], **H. Kuzmany**[3], **F. Hauke**[4], **A. Hirsch**[4], **J. Mende**[5], and **M. Mehring**[5]

[1] Budapest University of Technology and Economics, Institute of Physics, and Condensed Matter Research Group of the Hungarian Academy of Sciences, P.O. Box 91, 1521 Budapest, Hungary
[2] Institute of Physics of Complex Matter, FBS Swiss Federal Institute of Technology (EPFL), 1015 Lausanne, Switzerland
[3] Fakultät für Physik, Universität Wien, Strudlhofgasse 4, 1090 Wien, Austria
[4] Institut für Organische Chemie der Friedrich Alexander Universität Erlangen-Nürnberg, Henkestraße 42, 91054 Erlangen, Germany
[5] Physikalisches Institut, Universität Stuttgart, Pfaffenwaldring 57, 70569 Stuttgart, Germany

Received 8 June 2007, accepted 18 June 2007
Published online 26 September 2007

PACS 72.80.Rj, 73.63.Fg, 76.30.–v

$C_{59}N$ magnetic fullerenes inside single-wall carbon nanotubes (SWCNTs) are used to probe the density of states (DOS) on the host tubes using electron spin resonance (ESR). The $C_{59}N$ radicals are separated by C_{60} fullerenes to prevent dimerization and $C_{59}N–C_{60}$ heterodimers are formed at low temperatures. The electron spin–lattice relaxation time, T_1, of the heterodimers is deduced from the homogeneous ESR line-width. The analysis is supported by saturation ESR studies. The inverse of the heterodimer T_1 follows a linear behavior in the 20–300 K temperature range, the so-called Korringa law, evidencing a metallic DOS on all tubes in a bundle.

1 Introduction

Low energy excitation of single-wall carbon nanotubes (SWCNTs) can be studied with the help of magnetic resonance. It is neccessary to attach a spin probe to the tubes as the tubes are known to have no intrinsic ESR signal [1, 2]. Magnetic fullerenes, $N@C_{60}$ and $C_{59}N$ are ideal candidates for this purpose as fullerenes occupy preferentially the interior of the tubes, forming the "peapods" [3], and can be removed from the outside [4]. Encapsulation thus ensures that the local electron spins probe the properties of the tubes in analogy with nuclear magnetic resonance. We recently reported the encapsulation of $C_{59}N$ inside SWCNTs [5, 6]. As neighboring $C_{59}N$ molecules form ESR silent dimers, we separated them by adding C_{60} molecules so that C_{60} and $C_{59}N$ molecules enter the tubes together. It turns out that at low temperatures $C_{59}N$ and C_{60} form a bonded heterodimer molecule [7]. Measurements of the electron spin–lattice relaxation time, T_1 of the heterodimer is expected to yield information about the low energy excitations, i.e. about the vicinity of the Fermi surface of the host nanotubes.

Here, we report ESR measurements on the energetics of the heterodimer formation and on the measurement of the temperature dependence of T_1. We deduce T_1 from the homogeneous ESR line-width. The analysis is supported by direct time-domain and saturation ESR studies. The relaxation rate, $1/T_1$, follows the Korringa law and this is evidence for a metallic character of all SWCNTs in the bundles.

[*] Corresponding author: e-mail: ferenc.simon@univie.ac.at, Phone: +36 1 463 38 16, Fax: +36 1 463 38 19

2 Experimental

Synthesis of the current samples were reported previously [5]. In brief, we used commercial SWCNTs with suitable tube diameters to accommodate fullerenes. A mixture of functionalized and air-stable $C_{59}N$ derivatives and C_{60}'s were encapsulated with the solvent method [8]. ESR active $C_{59}N$ was obtained by heat treating the sample to remove the functional group. After this, the material is air sensitive and is sealed under He in quartz tubes. ESR and saturation ESR studies were performed on a Bruker Elexsys X-band spectrometer. We also prepared $C_{59}N$ embedded in the C_{60} crystal as a reference material, which we call crystalline material to distinguish from the peapod $C_{59}N$. Relaxation times were measured on the crystalline material with spin-echo ESR on a Bruker W-band pulsed spectromer.

3 Results and discussion

At room temperature, the ESR signal of $C_{59}N:C_{60}$@SWCNT consists of two components: a triplet structure corresponding to rotating $C_{59}N$ monomers and a singlet line corresponding to the static $C_{59}N{-}C_{60}$ heterodimer molecules [5]. The spectra, its temperature evolution, and the deconvolution to the triplet and singlet lines are shown in the inset of Fig. 1a. Clearly, the heterodimer dominates the low temperature spectrum and vanishes at higher temperatures. The coexistence and the temperature dependence of the two signals was understood for crystalline $C_{59}N:C_{60}$ as a thermal equilibrium between the ground state heterodimer and the rotating $C_{59}N$ monomers [7]. The heterodimer signal intensity normalized to the total (heterodimer + triplet) intensity gives the heterodimer concentration and is shown in Fig. 1. Similarly to crystalline $C_{59}N:C_{60}$ [7], the heterodimer concentration can be fitted with

$$\frac{I_{C_{59}N-C_{60}}}{I_{\text{total}}} = \frac{1}{1+e^{-\Delta F/k_B T}}, \tag{1}$$

where k_B is Boltzmann's constant and $\Delta F = E_a - T\,\Delta S$ with E_a being the binding energy of the heterodimer and ΔS being the entropy difference between the rotating monomer and the static heterodimer

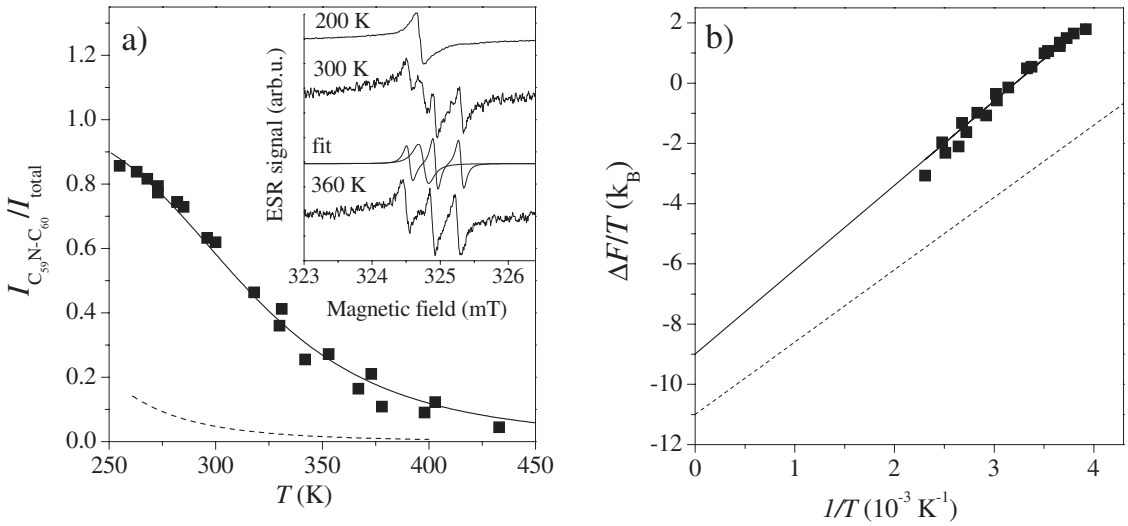

Fig. 1 a) Concentration of $C_{59}N{-}C_{60}$ bound heterodimers in $C_{59}N:C_{60}$@SWCNT. Inset shows the evolution of the spectra with the temperature. The deconvolution of the 300 K spectrum is also shown. b) The temperature normalized free energy difference, $\Delta F/T$ between the heterodimer and the monomer in units of k_B. Solid curves in both figures are fits with parameters explained in the text. Dashed curves show the respective quantities for crystalline $C_{59}N:C_{60}$ above the 261 K phase transition.

states. The relation described by Eq. (1) between the heterodimer concentration and the free energy difference allows to determine the temperature dependence of the temperature normalized free energy difference, $\Delta F/T$, which is shown in Fig. 1b in units of k_B. Clearly, a linear relationship between $\Delta F/T$ and $1/T$ with a non-zero crossing at $1/T$ is observed. This shows that the above model of the heterodimer concentration, that is described by Eq. (1), is correct and that it is neccessary to invoke an entropy difference between the two states of $C_{59}N$ in addition to the binding energy.

A fit with Eq. (1) for the peapod material is shown in Fig. 1a as a solid curve and gives $E_a(\text{peapod}) = 2800(200)$ K and $\Delta S(\text{peapod}) = 9(1)$. This compares to the results for the crystalline material with $E_a(\text{cryst}) = 2400(600)$ K and $\Delta S(\text{cryst}) = 11(2)$ [7]. The higher heterodimer concentrations for the peapod material is caused by the larger E_a and smaller ΔS values. The latter is explained by the limited rotational freedom of encapsulated $C_{59}N$. The same fits appear as lines for $\Delta F/T$ in Fig. 1b.

In analogy to NMR spectroscopy, the ESR spin–lattice relaxation time, T_1, of the localized heterodimer spins yields information on the electronic structure of the host SWCNT material [9]. ESR T_1 can be measured using several methods depending on the system investigated. The time-resolved spin-echo ESR yields a direct measurement of T_1, however it is limited to spin–lattice and spin–spin relaxation times (T_2) longer than a few μs. Shorter T_1's of a few hundred nanoseconds can be measured using continuous wave ESR spectroscopy from the line-width, ΔH, by separating the homogeneous, relaxation related line-width from the inhomogeneous one. Relaxation times between the micro and hundred nanoseconds domain can be measured using the so-called saturation ESR but this method has a limited precision to provide absolute T_1 values. T_1 of the crystalline material is sufficiently long to enable spin-echo measurements. However, as we show below, T_1 of the heterodimer spins in the peapod material lies in the few hundred nanosecond domain, where T_1 can be measured from the homogeneous broadening and saturation ESR can be used to check for the consistency of the values obtained.

In Fig. 2a, we show ΔH for the heterodimer signal as determined from fits with derivative Lorentzian lines. Clearly, ΔH has a temperature dependent component in addition to a $\Delta H_0 = 0.089(2)$ mT residual line-width, which is obtained by averaging the line-widths below 50 K. The line-shape of the heterodimer signal does not change with temperature, which indicates a uniform, homogeneous broadening in addition to the inhomogeneous residual width.

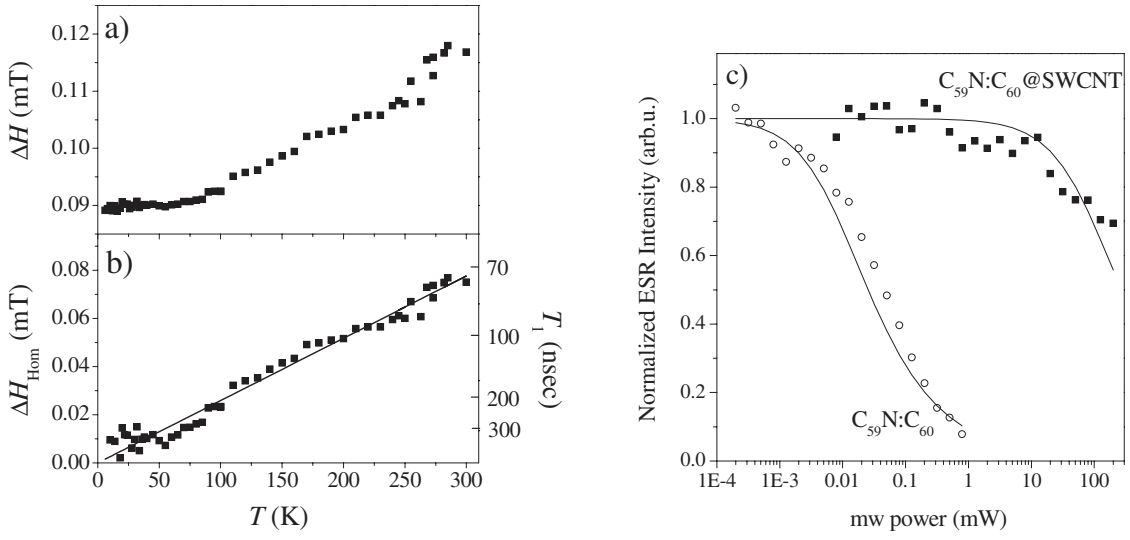

Fig. 2 a) Temperature dependence of the ESR line-width for the heterodimer signal. b) The homogeneous line-width with a linear fit (solid line). Corresponding T_1's are shown on the right axis. c) Saturation curves for crystalline $C_{59}N:C_{60}$ at 260 K and peapod $C_{59}N:C_{60}$@SWCNT at 20 K. Solid curves show the calculated saturated ESR intensities as explained in the text.

To obtain the homogeneous line-width, ΔH_{Hom}, we subtracted ΔH_0 from the line-width data: $\Delta H_{\mathrm{Hom}} = \sqrt{\Delta H^2 - \Delta H_0^2}$. Figure 2b shows ΔH_{Hom} and $1/T_1 = \gamma_e \Delta H_{\mathrm{Hom}}$, where $\gamma_e/2\pi = 28.0$ GHz/T is the electron gyromagnetic ratio.

To check the consistency of the measurement of T_1 from the homogeneous line-width, we performed saturated ESR measurements. In this method, the ESR signal intensity is progressively saturated upon increasing microwave power and the ESR signal intensity follows [9, 10]:

$$S(p) \propto \frac{\sqrt{p}}{\sqrt{1 + C\gamma^2 p T_1 T_2}} \tag{2}$$

where p is the microwave power, T_2 is the spin–spin relaxation time of the individual spin-packets, and C is a constant which depends on the microwave cavity and describes how large microwave magnetic field, $H_1 = \sqrt{Cp}$, is produced for a power of p. For the TE011 cavity with a quality factor of $Q = 4000$, $C = 1.59 \times 10^{-8}$ T^2/W [11]. In Fig. 2c, we show the saturation curves, $S(p)/\sqrt{p}$, normalized by the lowest power signal intensities for the crystalline $C_{59}N{:}C_{60}$ at 260 K and for the peapod $C_{59}N{:}C_{60}$@SWCNT at 20 K. Clearly, the ESR signal of the heterodimer saturates at much larger microwave powers for the peapod material indicating a much shorter relaxation time, which is attributed to the interaction of the heterodimer spins and the tubes.

Solid curves using Eq. (2) for the crystalline and peapod materials are shown with the T_1 and T_2 value in Table 1. $T_{1,2}$ were measured for the crystalline material using spin-echo ESR for the crystalline sample. For the peapod material, we took the $T_1 \approx 300$ ns from the homogeneous line-width analysis and assumed the equality of T_1 and T_2 due to the very short T_1. The calculated and measured saturation ESR data show a reasonable agreement for both the crystalline and the peapod material. This, on one hand shows that the saturation ESR measurement is compatible with the T_1 and T_2 values determined in the spin-echo experiment on the crystalline sample. On the other hand, it proves that the measurement of T_1 from the line-width for the peapod material is correct.

Now, we discuss the temperature dependence of the spin–lattice relaxation time. The most important property of $1/T_1$ is its linear T dependence in the 20–300 K temperature range. Below 20 K, the homogeneous broadening becomes too small to enable the measurement of T_1. The linear relation can be fitted with $(T_1T)^{-1} = 4.2(2) \times 10^4 (\mathrm{sK})^{-1}$ (fit shown in Fig. 2b). This suggests that Korringa relaxation, i.e. the interaction with conduction electrons [9] gives the relaxation of the heterodimer. An effective coupling constant (averaged for tube chiralities), J, of localized spins and conduction electrons is 11 meV as determined from the Korringa relation [9]:

$$\frac{1}{T_1 T} = \left(\frac{4\pi k_B}{\hbar}\right) J^2 \bar{n}(E_F)^2 \tag{3}$$

where $\bar{n}(E_F) = 0.014$ states/eV/atom is the DOS at the Fermi level for a $d \approx 1.4$ nm metallic tube in the tight-binding approximation [12]. The above discussed uniformity of the homogeneous broadening suggests that the heterodimer spins do not sense separate metallic and semiconducting tubes as it would be expected based on the geometry of tubes alone [12]. This can be explained by charge transfer in the SWCNTs bundles, which shifts the Fermi level and renders all tubes metallic, however there is a clear need for further experiments and theoretical studies in this respect.

Table 1 Spin–lattice and spin–spin relaxation times for the crystalline and peapod materials used to calculate the saturated ESR data.

	T_1	T_2
crystalline $C_{59}N{:}C_{60}$ (260 K)	120 µs	2 µs
peapod $C_{59}N{:}C_{60}$@SWCNT (20 K)	300 ns	300 ns

4 Summary

$C_{59}N$ magnetic fullerenes inside single-wall carbon nanotubes (SWCNTs) are used to probe the density of states (DOS) on the host tubes using electron spin resonance (ESR). The $C_{59}N$ radicals are separated by C_{60} fullerenes to prevent dimerization and $C_{59}N-C_{60}$ heterodimers are formed at low temperatures. The electron spin–lattice relaxation time, T_1, of the heterodimers is deduced from the homogeneous ESR line-width. The analysis is supported by saturation ESR studies. The inverse of the heterodimer T_1 follows a linear behavior, the so-called Korringa law, evidencing a metallic DOS on all tubes in a bundle.

Acknowledgements This work was supported by the Austrian Science Funds (FWF) project Nr. I83-N20 (ESF-IMPRESS), by the Hungarian State Grants (OTKA) No. TS049881, F61733 and NK60984, by the Deutsche Forschungsgemeinschaft (DFG). FS acknowledges the Zoltán Magyary and the Bolyai postdoctoral fellowships. Work in Lausanne was supported by the Swiss NSF and the European Research Network IMPRESS.

References

[1] A. S. Claye, N. M. Nemes, A. Jánossy, and J. E. Fischer, Phys. Rev. B **62**, 4845–4848(R) (2000).
[2] J.-P. Salvetat, T. Fehér, C. L'Huillier, F. Beuneu, and L. Forró, Phys. Rev. B **72**(1–6), 075440 (2005).
[3] B. W. Smith, M. Monthioux, and D. E. Luzzi, Nature **396**, 323–324 (1998).
[4] H. Kataura, Y. Maniwa, T. Kodama, K. Kikuchi, K. Hirahara, K. Suenaga, S. Iijima, S. Suzuki, Y. Achiba, and W. Krätschmer, Synth. Met. **121**, 1195/1196 (2001).
[5] F. Simon, H. Kuzmany, B. Náfrádi, T. Fehér, L. Forró, F. Fülöp, A. Jánossy, A. Rockenbauer, L. Korecz, F. Hauke, and A. Hirsch, Phys. Rev. Lett. **97**(1–4), 136801 (2006).
[6] F. Simon, H. Kuzmany, F. Fülöp, A. Jánossy, J. Bernardi, F. Hauke, and A. Hirsch, phys. stat. sol. (b) **2430**, 3263–3267 (2006).
[7] A. Rockenbauer, G. Csányi, F. Fülöp, S. Garaj, L. Korecz, R. Lukács, F. Simon, L. Forró, S. Pekker, and A. Jánossy, Phys. Rev. Lett. **94**, 066603 (2005).
[8] F. Simon, H. Kuzmany, H. Rauf, T. Pichler, J. Bernardi, H. Peterlik, L. Korecz, F. Fülöp, and A. Jánossy, Chem. Phys. Lett. **383**, 362–367 (2004).
[9] C. P. Slichter, Principles of Magnetic Resonance, 3rd ed. (Spinger-Verlag, New York, 1996).
[10] A. M. Portis, Phys. Rev. **91**, 1071 (1953).
[11] C. P. Poole, Electron Spin Resonance (John Wiley & Sons, New York, 1983).
[12] M. S. Dresselhaus, G. Dresselhaus, and Ph. Avouris, Carbon Nanotubes: Synthesis, Structure, Properties, and Applications (Springer, Berlin/Heidelberg/New York, 2001).

